Electronic Supplementary Material (ESI) for Journal of Materials Chemistry B.
This journal is The Royal Society of Chemistry 2016

Supporting Information

Construction of blood compatible lysine-immobilized chitin/carbon nanotubes microspheres and potential applications for blood purified therapy

Shuangquan Wu,[a,b] Bo Duan,[a] Xianpeng Zeng,[b] Ang Lu,[a] Xiaojuan Xu,[a] Yanfeng Wang,[*b] Qifa Ye,[*b] Lina Zhang[*a,c]

[a] College of Chemistry & Molecule Sciences, Wuhan University, Wuhan 430072, P. R. China

[b] Zhongnan Hospital of Wuhan University, Institute of Hepatobiliary Diseases of Wuhan University, Transplant Center of Wuhan University, Hubei Key Laboratory of Medical Technology on Transplantation, Wuhan 430071, P. R. China

[c] School of Chemistry and Chemical Engineering, Guangxi University, Nanning 530004, China

* Corresponding authore-mail address: zhangln@whu.edu.cn; yqf_china@163.com; yanfengwang@whu.edu.cn.

Contents

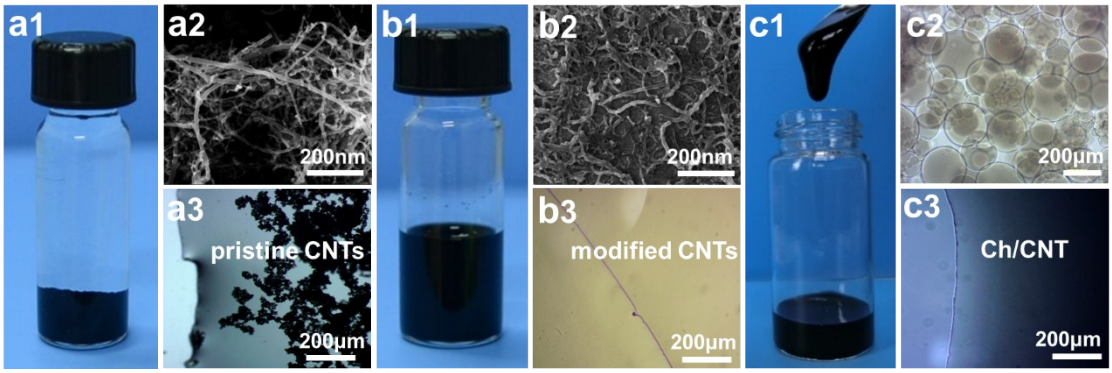

Fig. S1 (a1) Photograph of the pristine CNTs precipitated in water, (a2) SEM image of pristine CNTs, (a3) optical microscopy image of the pristine CNTs agglomerated in water, (b1) photograph of modified CNTs aqueous suspension (0.125mg/ml), (b2) SEM image of modified CNTs, (b3) optical microscopy image of homogenous modified CNTs aqueous solution, (c1) photograph of Ch/CNT homogeneous solution, (c2) optical microscopy image of Ch/CNT microspheres and (c3) optical microscopy image of Ch/CNT homogeneous solution.

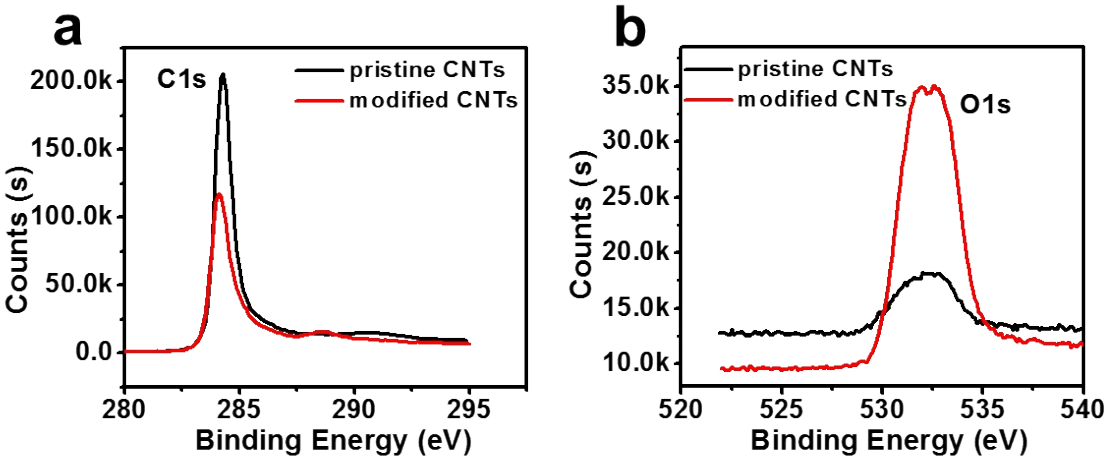

57

58 **Fig. S2** XPS spectra of C1s (a) and O1s (b) for pristine CNTs and modified CNTs, respectively.

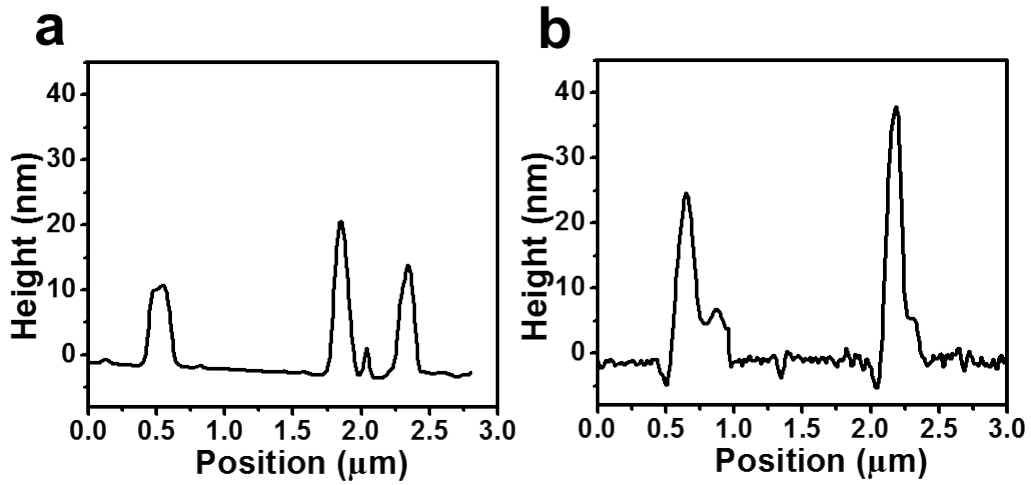

Fig. S3 Line profiles along the lines marked in the AFM images of modified CNTs (a) and Ch/CNT (b)

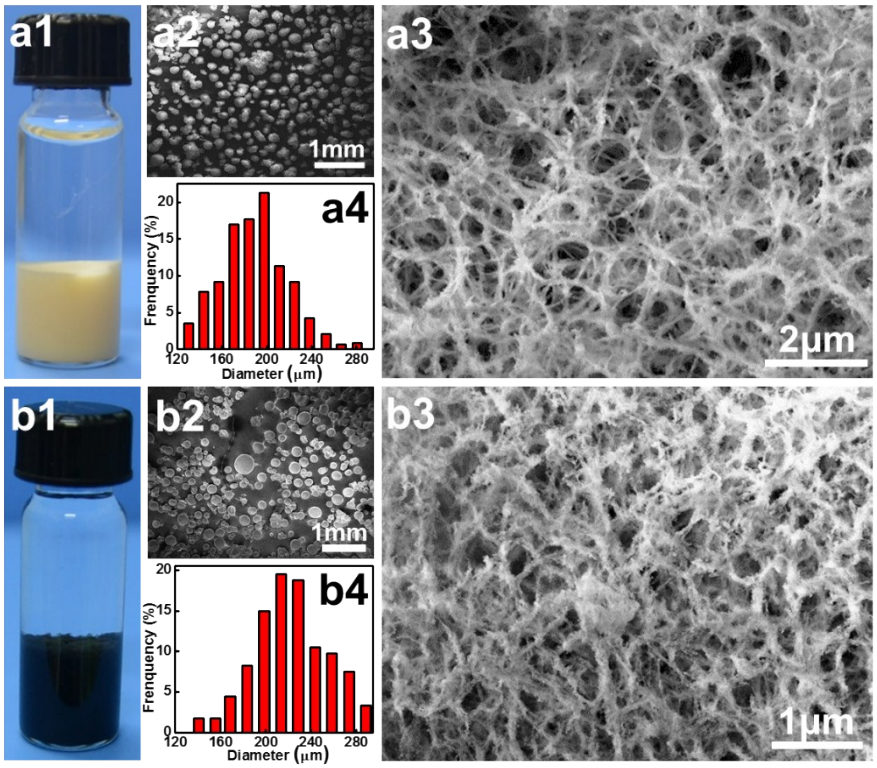

Fig. S4 (a1) Photograph of Ch/Lys microspheres, (a2, a3) SEM images of Ch/Lys microspheres, (a4) size distribution of Ch/Lys microspheres, (b1) photograph of Ch/CNT/Lys microspheres, (b2, b3) SEM images of Ch/CNT/Lys microspheres and (b4) size distribution of Ch/CNT/Lys microspheres.

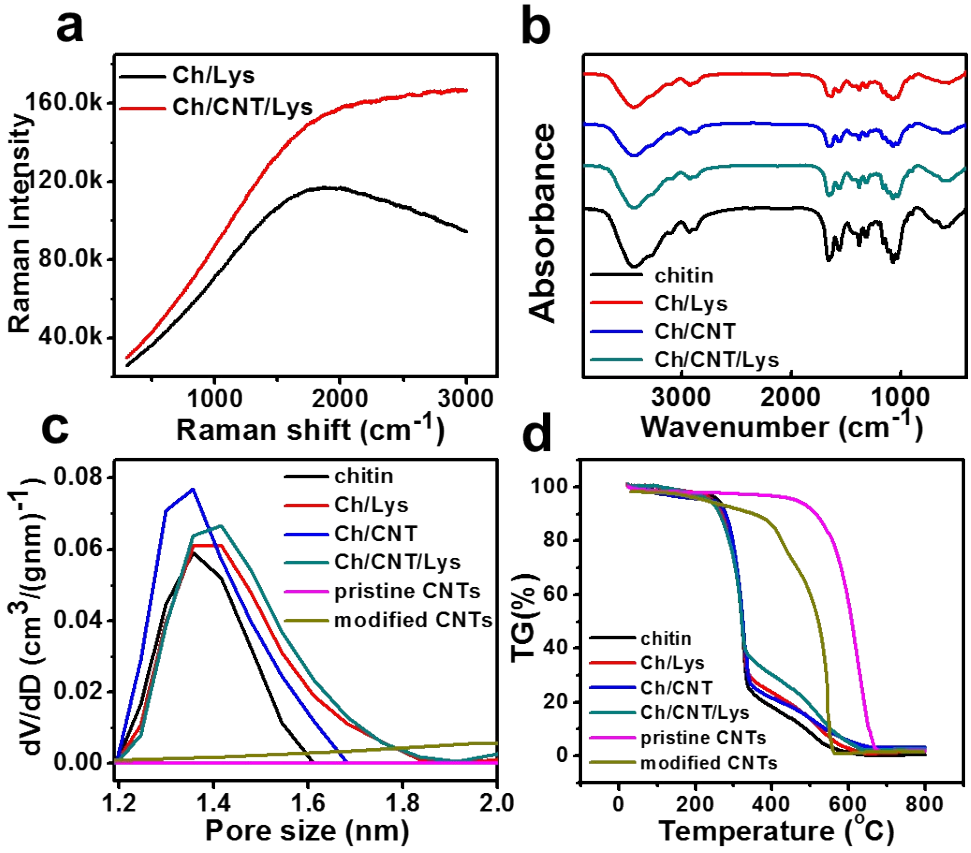

70

71 **Fig. S5** (a) Raman spectroscopy of Ch/Lys and Ch/CNT/Lys microspheres, (b) FT-IR spectra, (c)
72 pore size distribution determined by the DFT method and (d) TG curves of chitin-based
73 microspheres and CNTs.

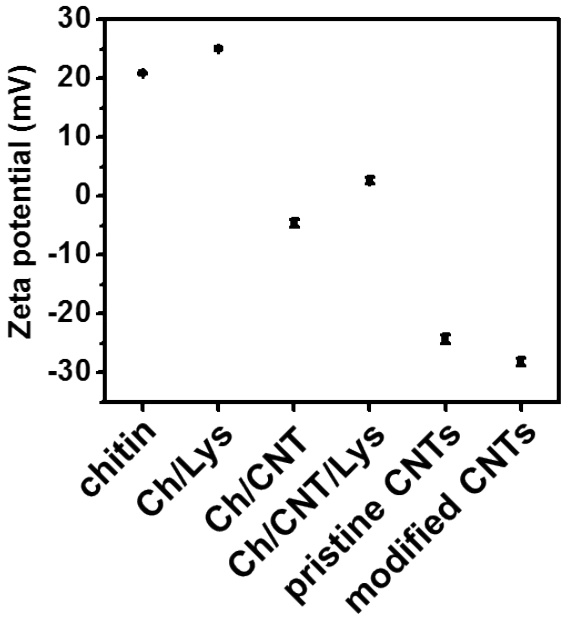

75

76 **Fig. S6** Zeta-potential of chitin-based microspheres and CNTs.

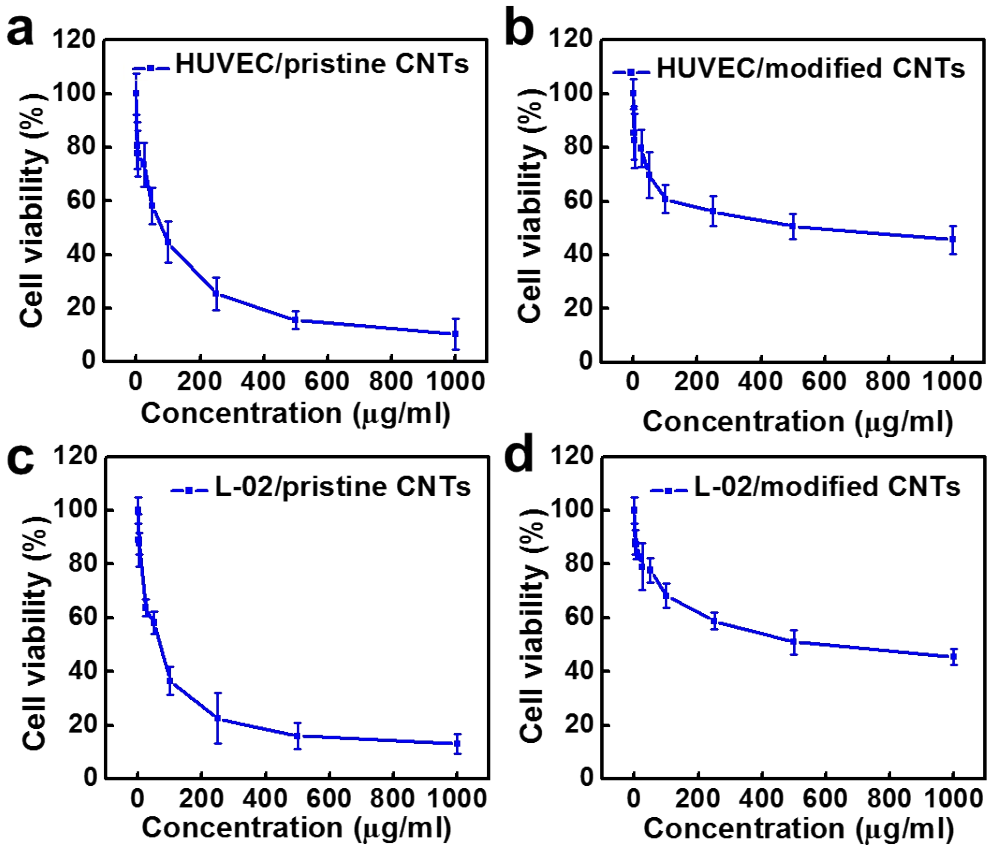

78

79 **Fig. S7** (a) In vitro cytotoxicity tests of different concentration of pristine CNTs incubated with
80 HUVEC cells, (b) different concentration of modified CNTs incubated with HUVEC cells, (c)
81 different concentration of pristine CNTs incubated with L-02 cells and (d) different concentration
82 of modified CNTs incubated with L-02 cells. Data are expressed as mean ± SD (n=4).

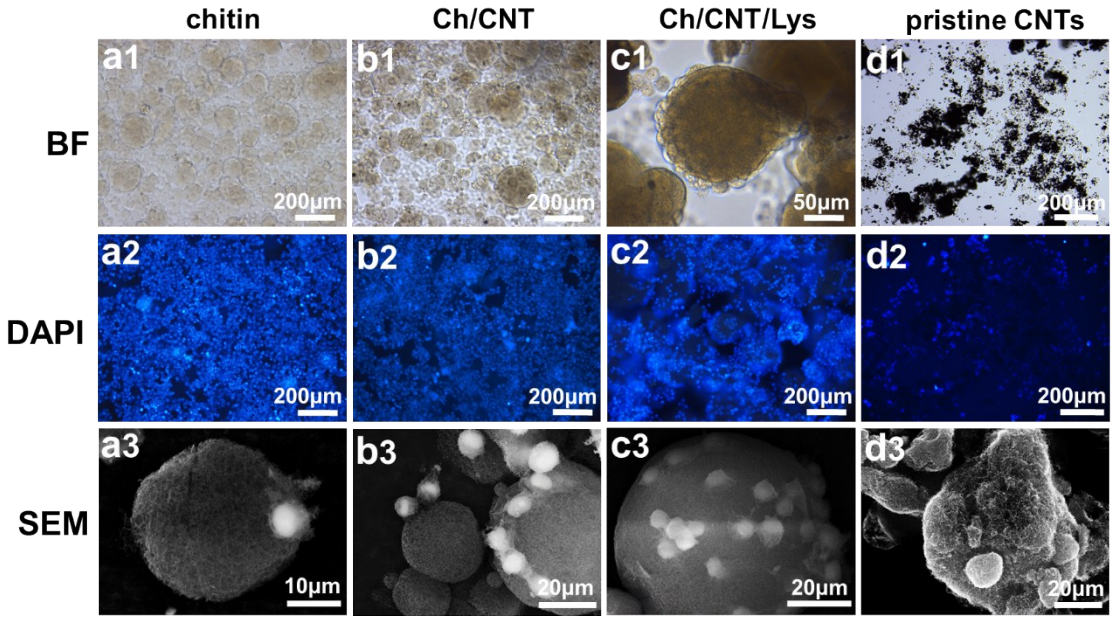

Fig. S8 Optical microscopy, fluorescence microscopy and SEM images of L-02 cells cultured on chitin microspheres (a), Ch/CNT microspheres (b), Ch/CNT/Lys microspheres (c) and pristine CNTs (d). The nuclei of the HUVEC cells were stained with 4′, 6-diamidino-2-phenylindole (DAPI).

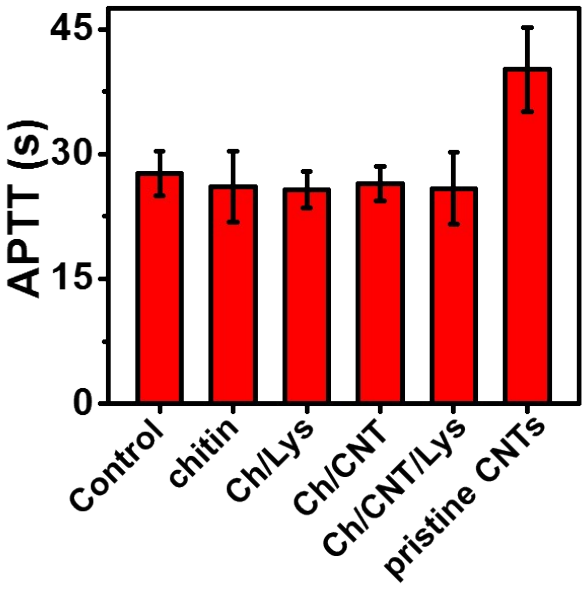

90

91 **Fig. S9** Activated partial thromboplastin time (APTT) of blood treated with microspheres and
92 pristine CNTs. Data are expressed as mean ± SD (n= 4).

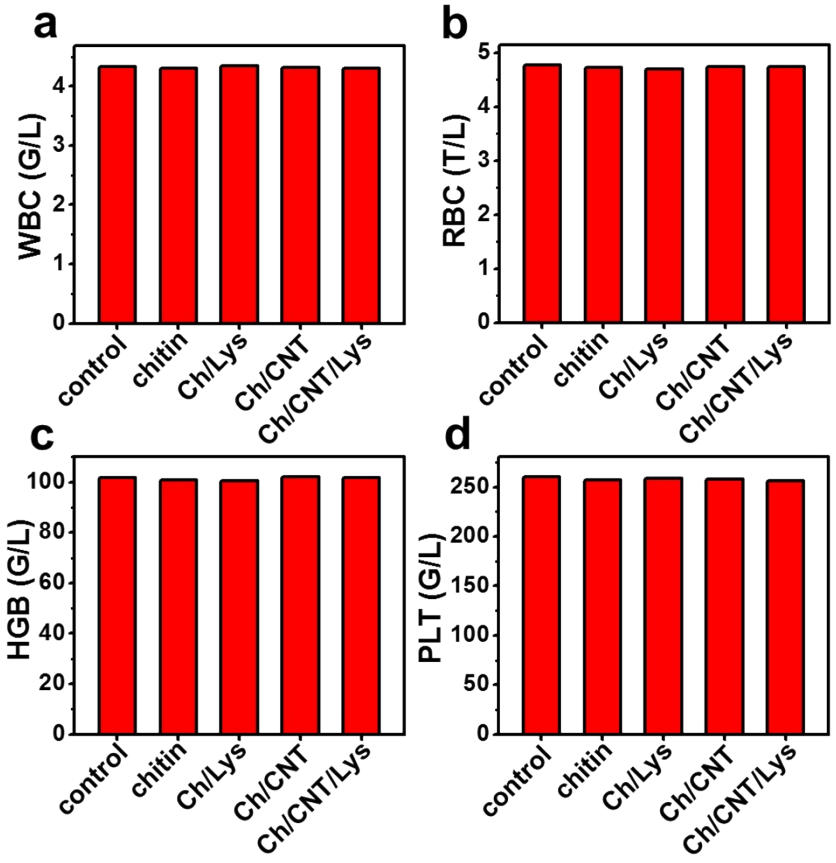

94

95 **Fig. S10** Changes in the blood content after treatment with chitin-based microspheres. (a) White
96 blood cell (WBC), (b) Red blood cell (RBC), (c) Hemoglobin (HGB) and (d) Platelet (PLT).

97

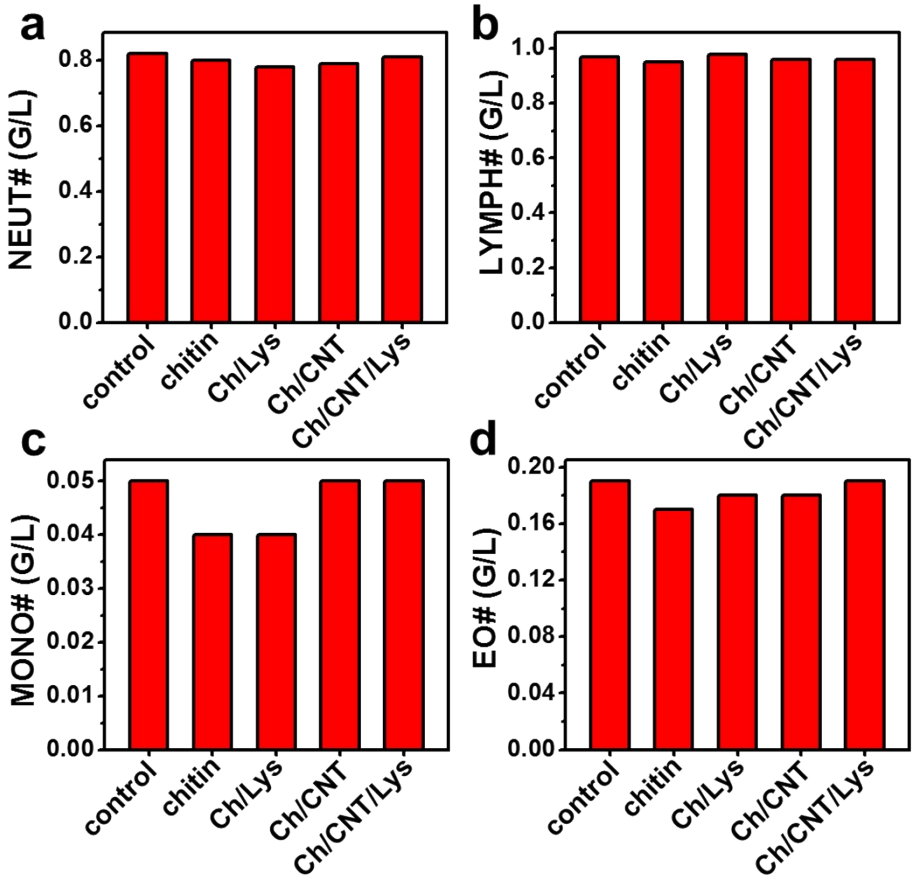

Fig. S11 Changes in the blood content after treatment with chitin-based microspheres. (a) Neutrophils (NEUT), (b) Lymphocyte (LYMPH), (c) Monocyte (MONO) and (d) Eosinophilia (EO).

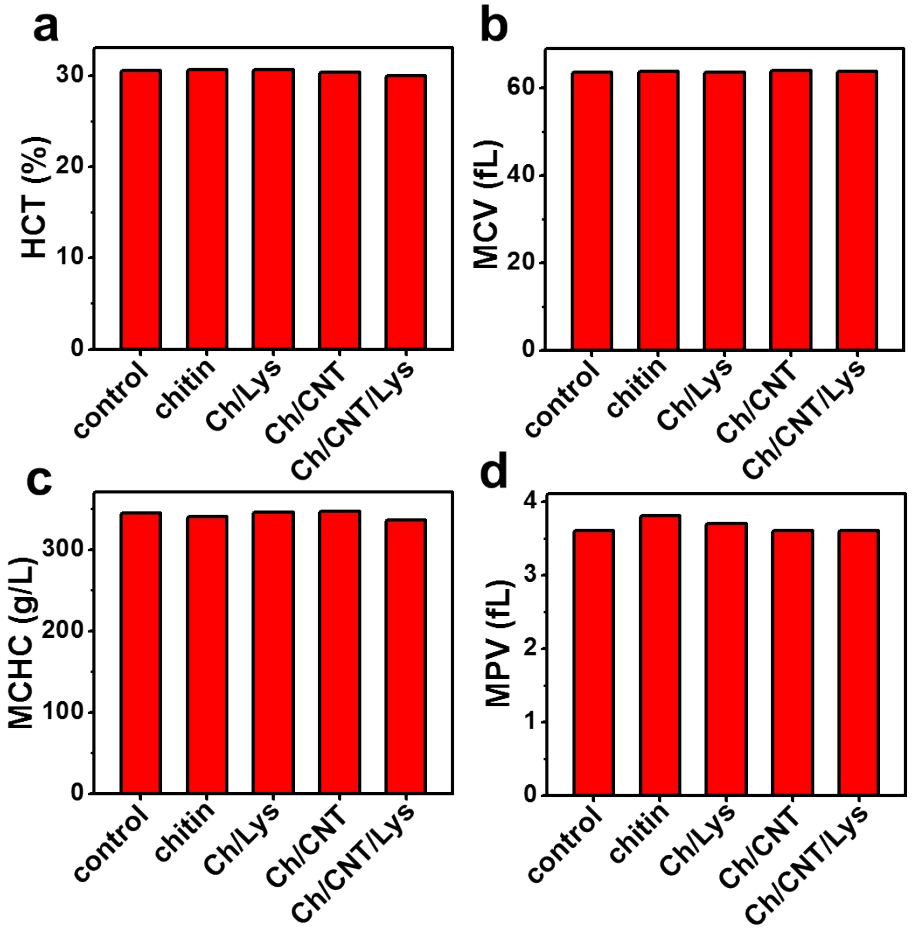

103

104 **Fig. S12** Changes in the blood content after treatment with chitin-based microspheres.
105 (a) Hematokrit (HCT), (b) Mean corpuscular volume (MCV), (c) Mean corpuscular
106 hemoglobin concentration (MCHC) and (d) Mean platelet volume (MPV).
107

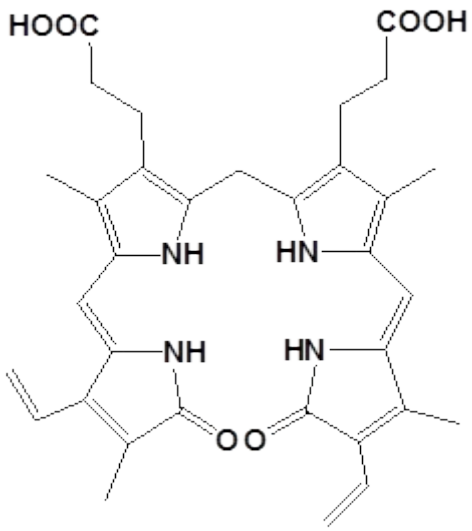

108

109 **Fig. S13** Chemical Structure of bilirubin. ($C_{33}H_{36}N_4O_6$, molar mass 584.66g/mol.).

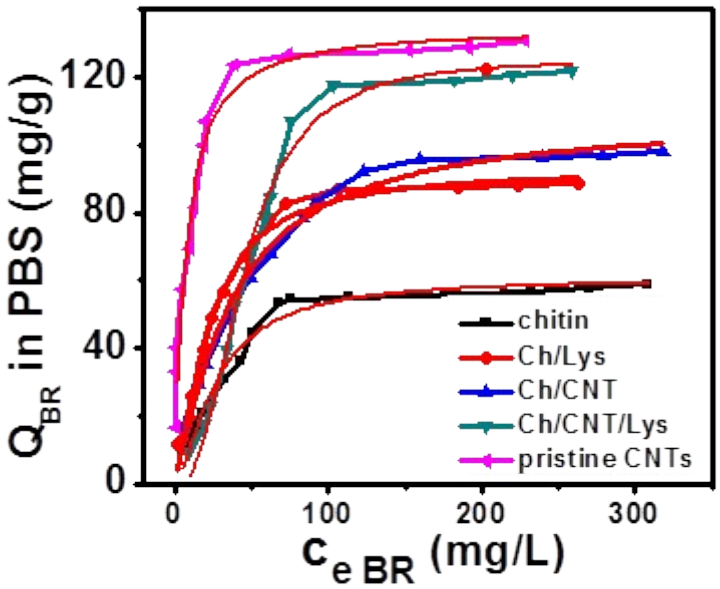

111

112 **Fig. S14** Langmuir isotherm of bilirubin adsorption capacity of chitin-based microspheres and
113 pristine CNTs in aqueous solution (PH=7.4).

115 **Table S1** The relative parameters of Langmuir model

Samples	Experiment	Langmuir		
	Q max(mg/g)	Q max-Langmuir (mg/g)	Standard Error	R^2
chitin	55.1	60.6	2.4	0.96
Ch/Lys	81.8	93.2	2.9	0.98
Ch/CNT	96.2	108.9	4.2	0.98
Ch/CNT/Lys	107.2	125.2	3.4	0.98
pristine CNTs	123.6	134.5	4.8	0.95

116

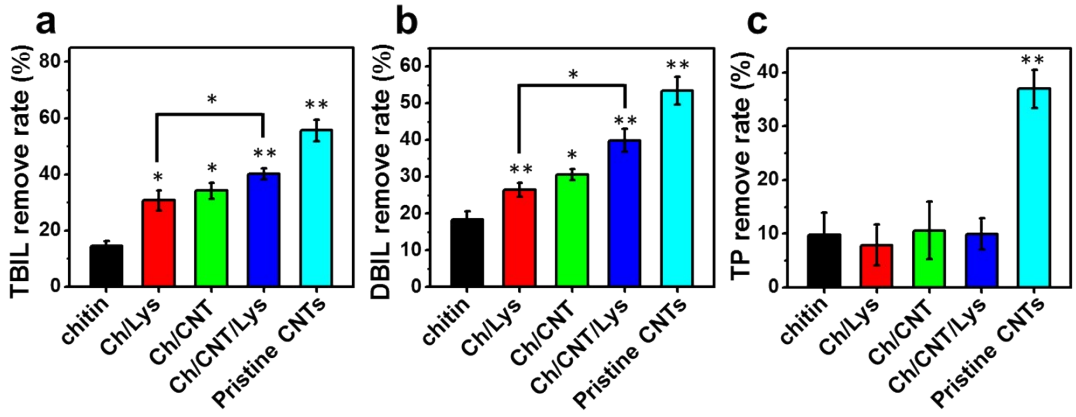

117

118 **Fig. S15** Removal rate of total bilirubin (TBIL) (a), direct bilirubin (DBIL) (b) and total protein
119 (TP) from plasma on the chitin-based microspheres and pristine CNTs. ($C_{0\ TBIL}$ = 55.1 μmol/L; C_{0}
120 $_{DBIL}$ = 42.2 μmol/L; $C_{0\ TP}$ =20.1 g/L,). Data are expressed as mean ± SD (n=4). The bars represent
121 SD. *p < 0.05, **p < 0.001, when compared with chitin microspheres. *p < 0.05 was considered
122 statistically significant.
123